

## Highly Branched Photomechanical Crystals

Rabih Al-Kaysi<sup>1\*</sup>, Fei Tong<sup>2</sup>, Maram Al-Haidar<sup>1</sup>, Lingyan Zhu<sup>2</sup>, Christopher J. Bardeen<sup>2\*</sup>

<sup>(1)</sup> College of Science and Health Professions-3124,  
King Saud bin Abdulaziz University for Health Sciences, and King Abdullah International  
Medical Research Center, Ministry of National Guard Health Affairs, Riyadh 11426,  
(Kingdom of Saudi Arabia)

<sup>(2)</sup> Department of Chemistry  
University of California, Riverside  
501 Big Springs Road  
Riverside, CA 92521 (USA)

\*E-mail: [christopher.bardeen@ucr.edu](mailto:christopher.bardeen@ucr.edu), [rabihalkaysi@gmail.com](mailto:rabihalkaysi@gmail.com), [kaysir@ksau-hs.edu.sa](mailto:kaysir@ksau-hs.edu.sa)

### General information

#### Synthesis of *tert*-butyl-4F9AC

#### Sample preparation and characterization using powder XRD and polarized light microscopy.

**Figure S1a:** <sup>1</sup>H-NMR spectrum of *tert*-butyl-4F9AC

**Figure S1b:** <sup>13</sup>C-NMR spectrum of *tert*-butyl-4F9AC

**Figure S1c:** HRMS of *tert*-butyl-4F9AC.

**Figure S1d:** IR spectrum of *tert*-butyl-4F9AC over KBr

**Figure S2.** Optical microscope images of 4F9AC crystals grown under different conditions

**Figure S3.** Scanning electron microscopy images of G1 and G3 4F9AC microcrystals

**Figure S4:** 4F9AC branched microcrystal viewed using a polarized light microscope

**Figure S5:** HPLC analysis of the branched 4F9AC microcrystals

**Figure S6:** PXRD of powdered branched 4F9AC microcrystals

**Figure S7.** Optical microscope images of highly branched 4F9AC microcrystals

**Figure S8.** Optical microscopy images of G1, G2 and G3 branched 4F9AC microcrystals

**Figure S9.** Optical microscopy images of 4F9AC microcrystals grown using increasing concentrations of 1-Dodecanol.

## General Information

All starting materials and reagents were purchased from Sigma-Aldrich. Dry benzene was prepared by distilling it over  $\text{CaH}_2$  and storing it over activated molecular sieves (3 Å).  $^1\text{H}$ -NMR and  $^{13}\text{C}$ -NMR spectra were recorded at 20 °C on a Varian Inova (three channel triple axis gradient spectrometer) at 500 MHz and 125.75 MHz, respectively. The probe for  $^1\text{H}$  and  $^{13}\text{C}$  is 5 mm triple resonance triple axis gradient. Chemical shifts were reported as  $\delta$  in (ppm) units relative to tetramethylsilane (TMS) internal standard ( $^1\text{H}$ -NMR: TMS = 0 ppm). Multiplicities were abbreviated as: s (singlet); d (doublet); t (triplet); dd (doublet of doublets); m (multiplet). Coupling constants  $J$  values were reported in Hz. HPLC analysis was performed on a Shimadzu (LC-20AD) using a general purpose BDS Hypersil C18 column (4.6×250 mm) from Thermo Scientific. An isocratic mobile phase was composed of 80% acetonitrile, 20% water with pH = 2.5 and a flow rate of 1.5 mL/min. The detector wavelength was set at 254 nm, and the column temperature at 35 °C. IR measurements were performed using an IR Affinity-1 FTIR from Shimadzu. SEM measurements were performed using a JEOL JSM-6510LV scanning electron microscope. Mass spectrometry measurements were performed using an Agilent Technologies 1200 Series instrument with a G1312A Binary Pump and a G1316A Thermostatted Column Compartment.

### **Synthesis of *tert*-butyl-4-fluoroanthracene-9-carboxylate (*tert*-butyl-4F9AC):**

A suspension of 4-fluoroanthracene-9-carboxylic acid (4F9AC, 99% pure, 0.1 g, 0.43 mmol) in dry benzene (5 mL) was prepared. Trifluoroacetic anhydride (99% pure, 0.5 mL, 1.8 mmol, 4 equivalence) was added drop wise while stirring at room temperature under argon gas. The carboxylic acid dissolved and the solution turned light yellow in color. Dry *tert*-butanol (99% pure, 0.13g, 1.8 mmol, 4 equivalents) was added to the mixture and stirred under argon gas for 3 hours. The reaction progress was monitored by thin layer chromatography (silica gel, methylene dichloride/hexanes). The organic layer was washed with 3×5 mL volumes of aqueous  $\text{K}_2\text{CO}_3$  solution (2 M) to remove any excess acid. The organic phase was dried over anhydrous  $\text{MgSO}_4$  before decanting it and removing the solvent under reduced pressure. A pale yellow crude product was obtained and recrystallized from hot ethanol to give pale yellow needles 0.067g (yield 55%). Melting point (uncorrected) 145-147 °C,  $^1\text{H}$ -NMR (500 MHz,  $\text{CDCl}_3$ )  $\delta$

(ppm) = 1.78 (s, 9H), 7.12-7.16 (dd,  $J=10$ , 5 Hz, 1H), 7.43 - 7.47 (m, 1H), 7.51-7.54 (m, 1H), 7.57-7.60 (m, 1H), 7.85 - 7.87 (d,  $J = 10$  Hz, 1H), 8.05-8.09 (t,  $J = 10$  Hz, 2H), 8.76 (s, 1H) (Figure S1a).  $^{13}\text{C}$ -NMR (125.75 MHz,  $\text{CDCl}_3$ )  $\delta$  (ppm) = 28.43 (*tert*-butyl methyl carbons), 81.39, 107.59-107.74 (d,  $J = 18.9$  Hz), 120.87-120.9 (d,  $J = 3.77$  Hz), 121.65-121.68 (d,  $J = 3.77$  Hz), 122.35-122.49 (d,  $J_{(\text{C-C-F})} = 17.61$  Hz), 124.86, 125.88, 125.93, 126.00, 127.39, 128.36, 128.97, 129.66-129.68 (d,  $J = 2.51$  Hz), 131.00, 157.77-159.80 (d,  $J_{(\text{C-F})} = 255.27$  Hz), 168.60 (C=O) (Figure S1b). High-resolution mass spectrometry (HRMS) (Figure S1c)  $m/z$ : calc. for  $\text{C}_{19}\text{H}_{17}\text{FNaO}_2$   $[\text{M} + \text{Na}]^+$  319.1105, found 319.1126, and for  $\text{C}_{19}\text{H}_{21}\text{FNO}_2$   $[\text{M} + \text{NH}_4]^+$  314.1551, found 314.16. IR (KBr):  $\nu$  ( $\text{cm}^{-1}$ ) = 3073(w), 3051(w), 2972(m), 1714(s), 1637(m), 1525(s), 1460(s), 1368(s), 1245(s), 1165(m), 1152(m), 1139(m), 964(m), 889(m) (Figure S1d).

### **Sample Preparation and Characterization**

To grow branched microcrystals, a solution of *tert*-butyl-4F9AC in acetonitrile (50 mM) was used to deposit  $\sim 1.0$  mg of the *tert*-butyl ester in a 20 mL reaction vial. The acetonitrile was evaporated under argon gas, leaving behind a thin polycrystalline film. A 10 mL aqueous solution of  $\text{H}_3\text{PO}_4$  (3.5 M), sodium dodecyl sulfate (SDS, 10 mM) and 1-dodecanol (1 mM) was added to the vial, resulting in a *tert*-butyl-4F9AC concentration of  $\sim 0.3$  mM. The resulting mixture was sonicated for a minute to disperse the ester film. The vial was fixed perpendicular to the rotational axis of a benchtop rotary laboratory mixer set at 8 rpm inside a large convection oven at  $35^\circ\text{C}$ . Mixing for 3 days resulted in a cloudy suspension of highly branched 4F9AC microcrystals.

To record the photomechanical response of the crystals, we used an Optika brand fluorescence microscope with a 100 W high pressure Hg lamp and fitted with a 365 nm bandpass filter. The UV intensity was measured using a radiometer equipped with a 365 nm sensor. The average UV output measured at the focus using a  $10\times$  magnification (3mm diameter spot) was  $\sim 30$  mW/cm $^2$ . A 2 megapixel camera (Optika) was used to record movies at 15 frames per second and still images at  $1600\times 1200$  pixel resolution. The microscope was placed in a room with an ambient temperature of  $32^\circ\text{C}$  in order to decrease the reset time of the photoreacted 4F9AC to just a few seconds. A drop of the

microcrystal suspension was placed on a glass slide, gently covered with a cover slip and allowed to settle before recording any measurements.

To prepare dry samples, several drops of the microcrystal suspension were filtered over a Whatman Anodisc inorganic filter membrane (13 mm diameter) with a nominal pore diameter of 200 nm. The residue was washed with deionized water and allowed to air dry. Powder X-ray diffraction data were collected on a Panalytical Empyrean X-ray powder diffractometer (CuK radiation,  $\lambda = 1.5406 \text{ \AA}$ , 45kV/40 mA power) at room temperature in the dark. Scanning electron microscopy (SEM) measurements were performed using a JEOL JSM-6510LV scanning electron microscope. Samples were sputter coated with a 5 nm thick layer of Pt prior to scanning. To obtain polarized light microscopy images, an Optika brand microscope was fitted with two polarizing filters rotated  $90^\circ$  to each other. The sample stage was rotated to view different birefringent arms of a given branched crystal.

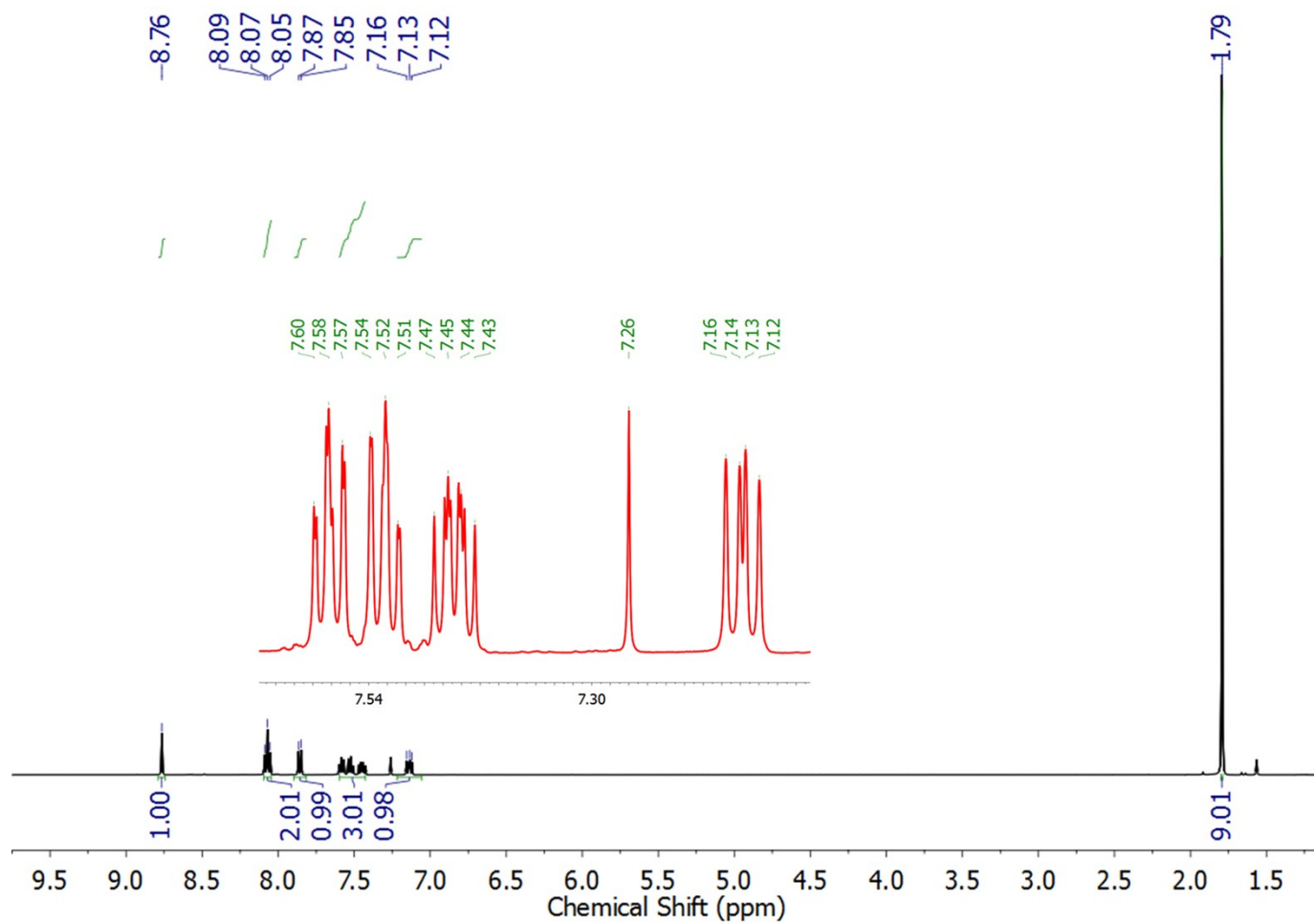


**Figure S1a.** <sup>1</sup>H-NMR of *tert*-butyl-4F9AC in CDCl<sub>3</sub> (Sigma-Aldrich, 99.9%+).

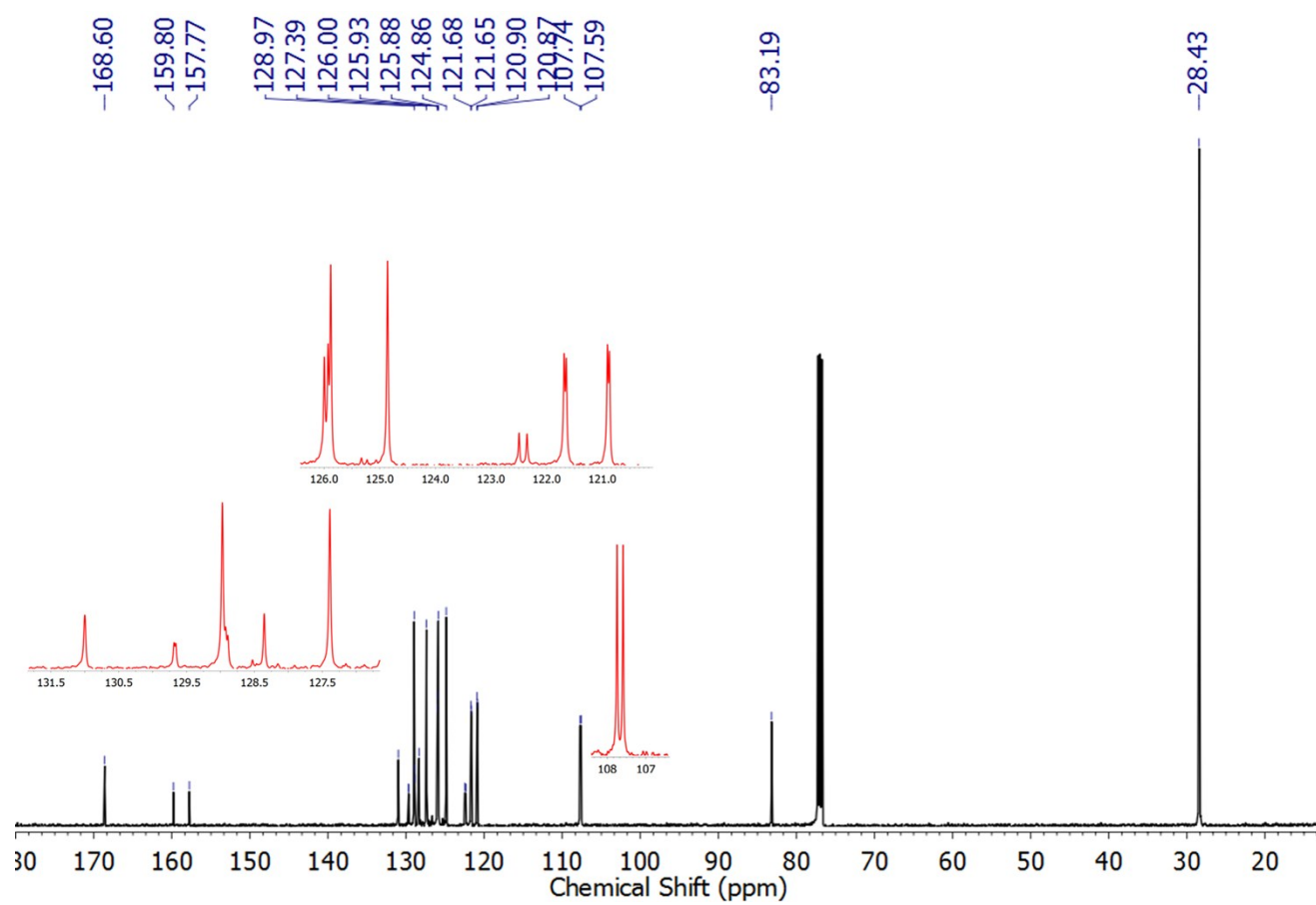


**Figure S1b.** <sup>13</sup>C-NMR of *tert*-butyl-4F9AC in CDCl<sub>3</sub> (Sigma-Aldrich, 99.9%+).

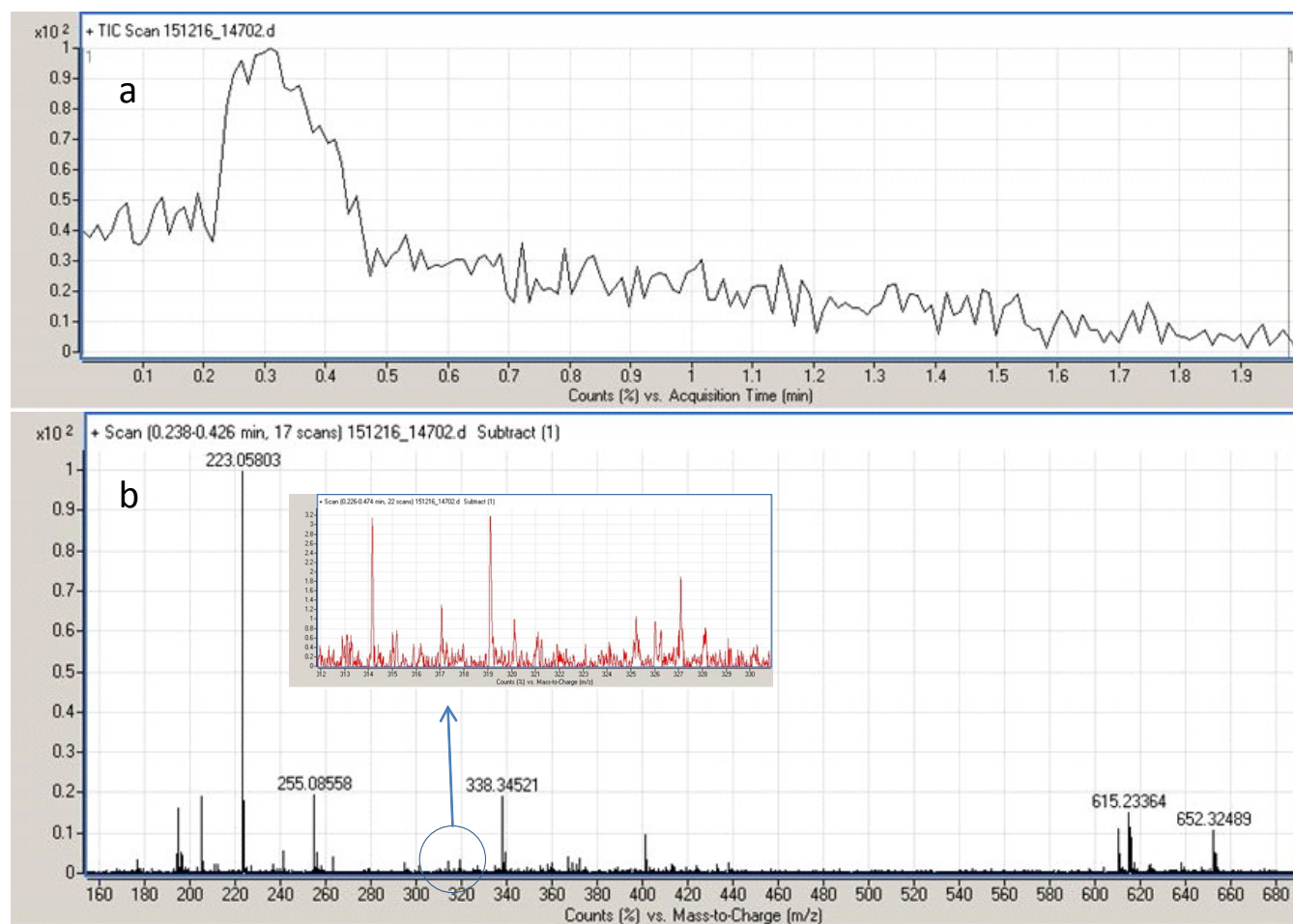


**Figure S1c:** High resolution mass spectrometry of *tert*-butyl-4F9AC obtained by dissolving 0.1 mg in 0.1 mL methanol (HPLC grade, ACS, 99.9 %+). a) LC chromatograph of the sample showing a single peak, indicating a single component in the sample. b) Mass spectrogram showing the parent peaks at  $[M + Na]^+ = 319.1126$  and fragmentations at 223.05803 (loss of  $(CH_3)_3O$ )

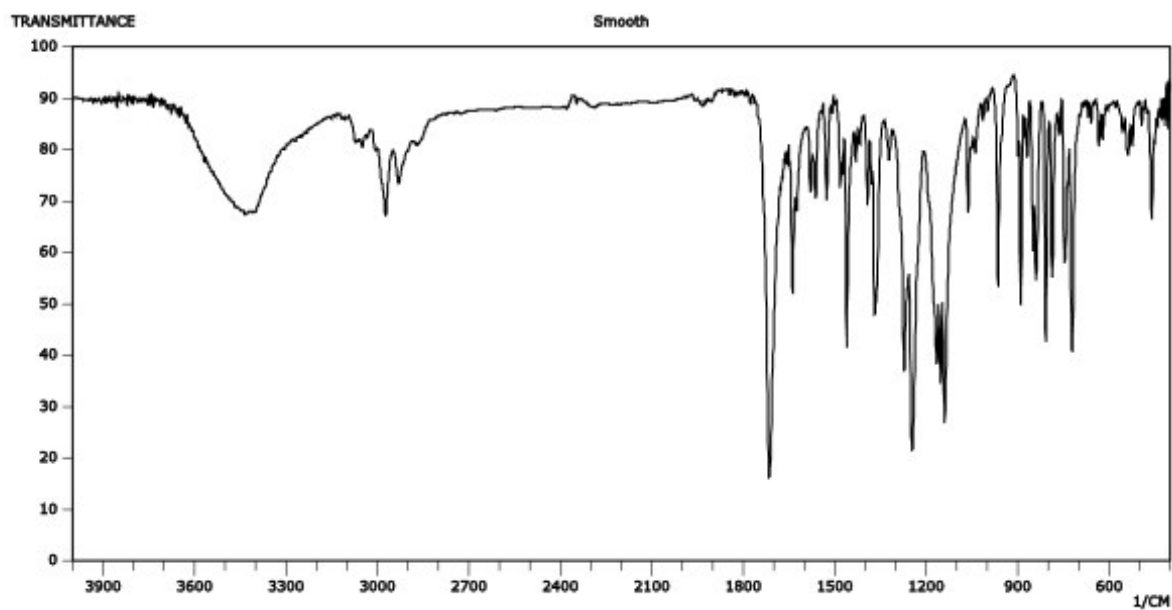


**Figure S1d.** IR spectrum of *tert*-butyl-4F9AC mixed with KBr. The broad peak between 3100 - 3600  $\text{cm}^{-1}$  is due to residual water in the KBr.





**Figure S2.** Optical microscopy images of 4F9AC crystals grown under different conditions in a solution containing  $[\text{H}_3\text{PO}_4] = 3.5 \text{ M}$ ,  $[\text{SDS}] = 10 \text{ mM}$ ,  $[\text{1-dodecanol}] = 1 \text{ mM}$  and  $[\text{tert-butyl-4F9AC}] = 0.3 \text{ mM}$ . (a) 4F9AC microribbons grown without agitation at  $35 \text{ }^\circ\text{C}$ , showing absence of branching. Scale bar =  $45 \text{ }\mu\text{m}$ . (b) Rarely observed, asymmetric 4F9AC microribbon clusters grown at  $35 \text{ }^\circ\text{C}$  without agitation. Scale bar =  $45 \text{ }\mu\text{m}$ . (c) Bundle of intertwined 4F9AC nanowires grown with agitation at a temperature close to  $100 \text{ }^\circ\text{C}$ . Scale bar =  $50 \text{ }\mu\text{m}$ .

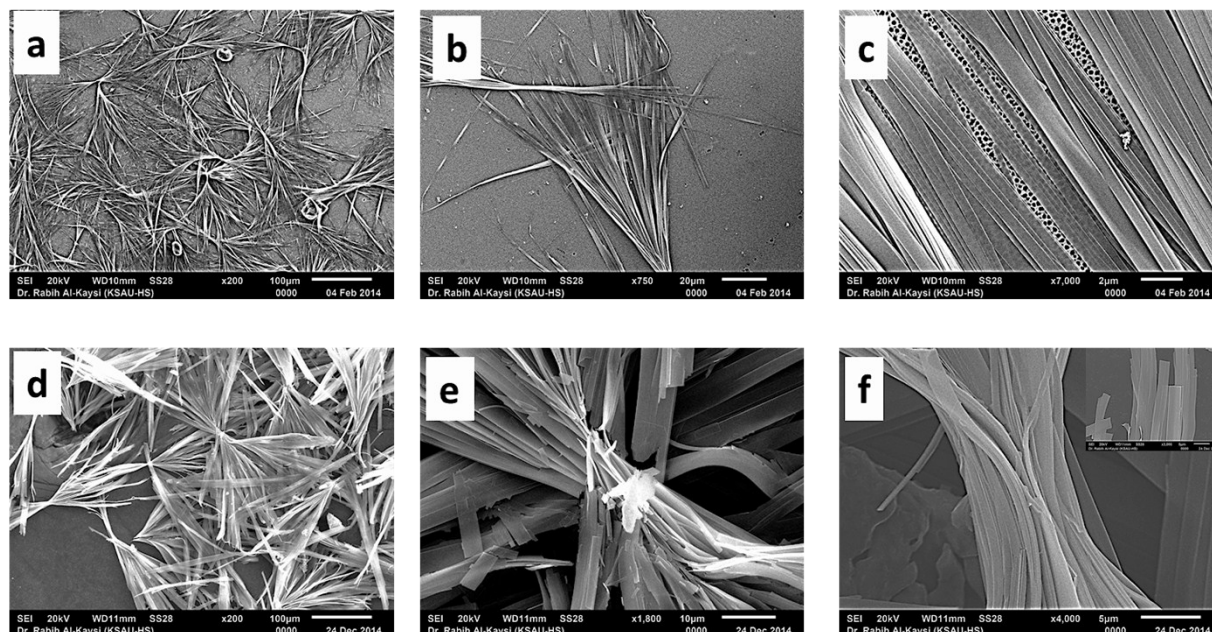


**Figure S3.** Scanning electron microscopy images of G1 and G3 branched microcrystals. (a), (b), and (c) SEM images with gradual magnification of a G1 branched 4F9AC microcrystal. (d), (e), and (f) SEM images with gradual magnification of a G3 branched 4F9AC microcrystal.

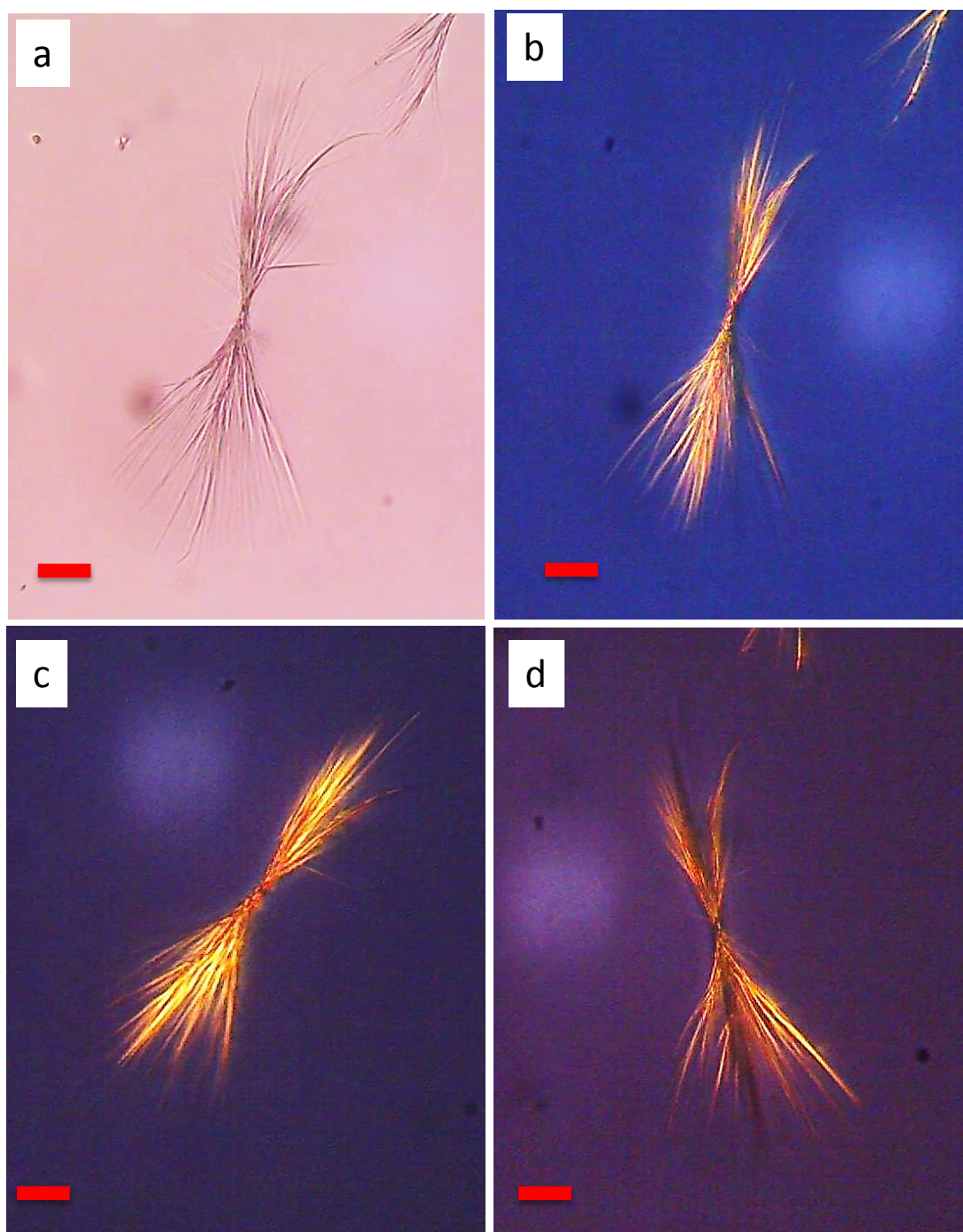


**Figure S4:** Optical microscopy images of a branched 4F9AC microcrystal under different polarization conditions. (a) No cross-polarized light. (b) Using crossed polarizers,  $0^\circ$  rotation of sample stage. (c) Sample stage rotated by  $+20^\circ$ . (d) Sample stage rotated by  $-30^\circ$ . Scale bars = 30  $\mu\text{m}$

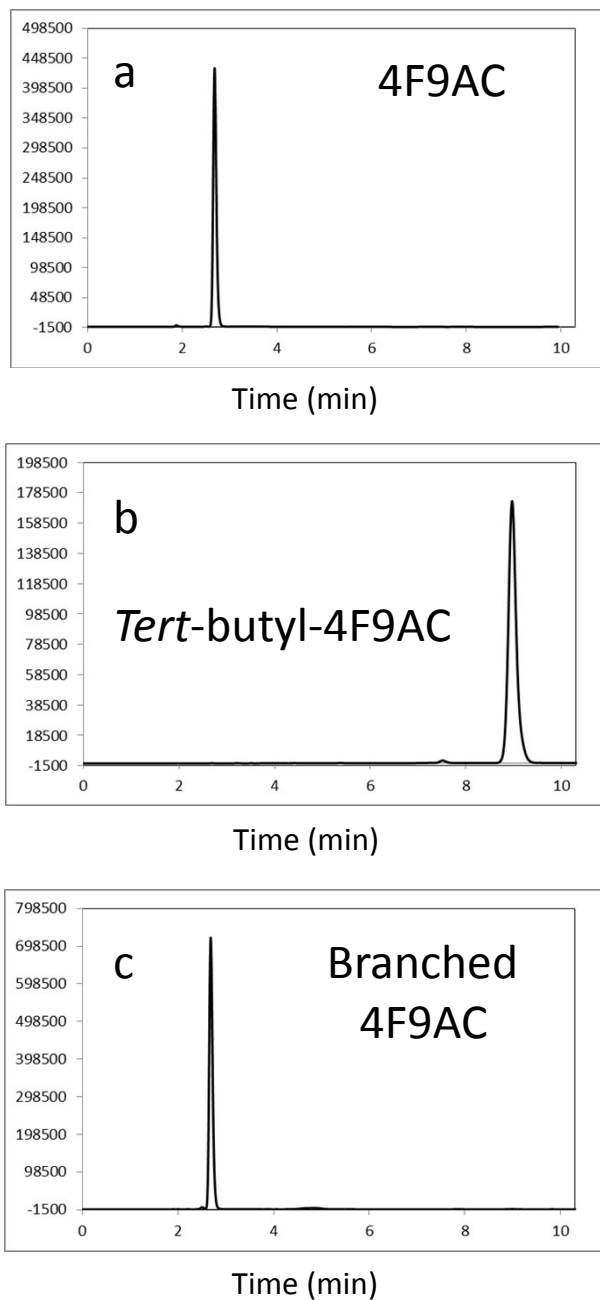


**Figure S5:** HPLC analysis of the branched 4F9AC microcrystals to confirm purity and identity of the crystals. A) HPLC of pure 4F9AC. b) HPLC of *tert*-butyl-4F9AC. c) HPLC of branched crystals after filtration and washing with deionized water. In all cases the 4F9AC crystals were dissolved in an isocratic mobile phase composed of 80% acetonitrile and 20% water (pH = 2.5)

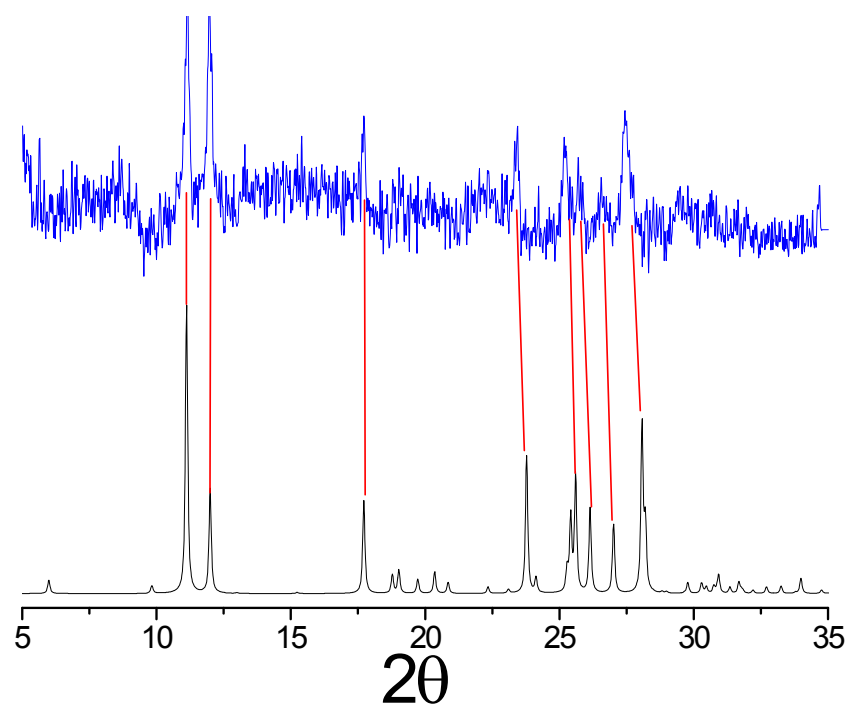


**Figure S6:** Comparison of PXRD data between powdered branched 4F9AC microcrystals (blue) and the PXRD pattern calculated from the single crystal data from reference 12 (black). The matching peaks indicate that the branched microcrystals have the same crystal structure as the bulk crystals and do not form a new polymorph.



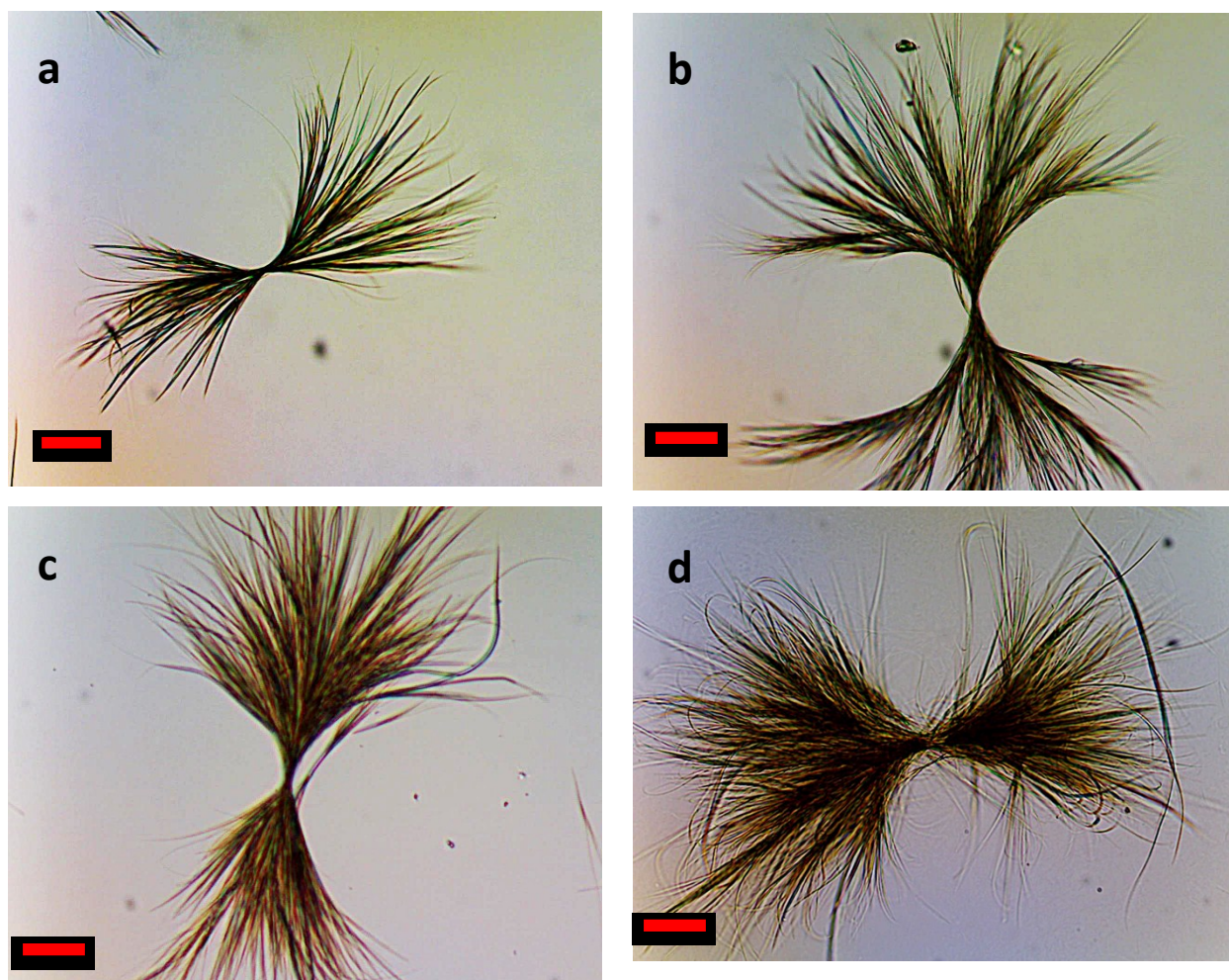


**Figure S7.** Optical microscope images of highly branched 4F9AC microcrystals prepared using different starting concentration of *tert*-butyl-4F9AC. Figures (a) → (d) show the results of increasing the initial concentration of *tert*-butyl-4F9AC. (a) ~ 0.2 mM. (b) 0.5 mM. (c) 1 mM. (d) > 2 mM, with some unhydrolyzed *tert*-butyl-4F9AC. Scale bar = 50  $\mu\text{m}$ .

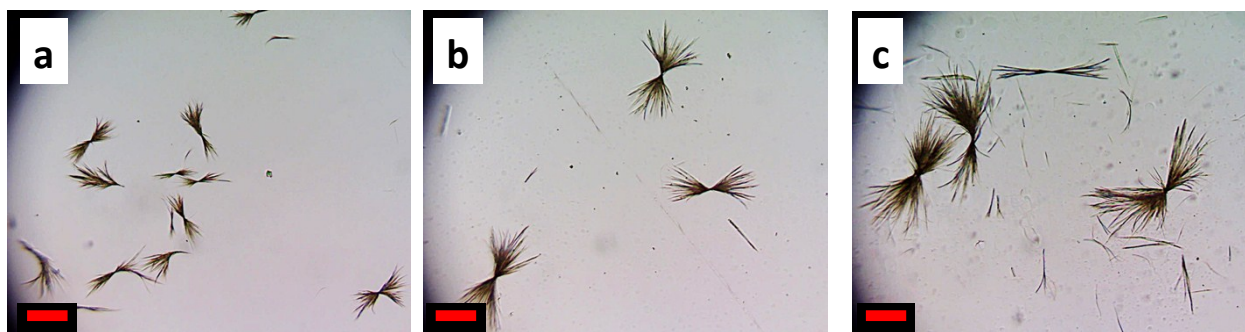


**Figure S8.** Optical microscopy images of seeded growth of branched 4F9AC microcrystals. (a) G1 branched microcrystals prepared using an initial [*tert*-butyl-4F9AC] = 0.3 mM followed by agitation at 35 °C. (b) G2 branched microcrystals prepared by adding enough *tert*-butyl-4F9AC to G1 to give a 0.3 mM concentration, then agitated at 35 °C again. (c) G3 branched microcrystals prepared by adding enough *tert*-butyl-4F9AC to G2 to give a 0.3 mM concentration, then agitated at 35 °C again. Scale bars = 150  $\mu$ m.

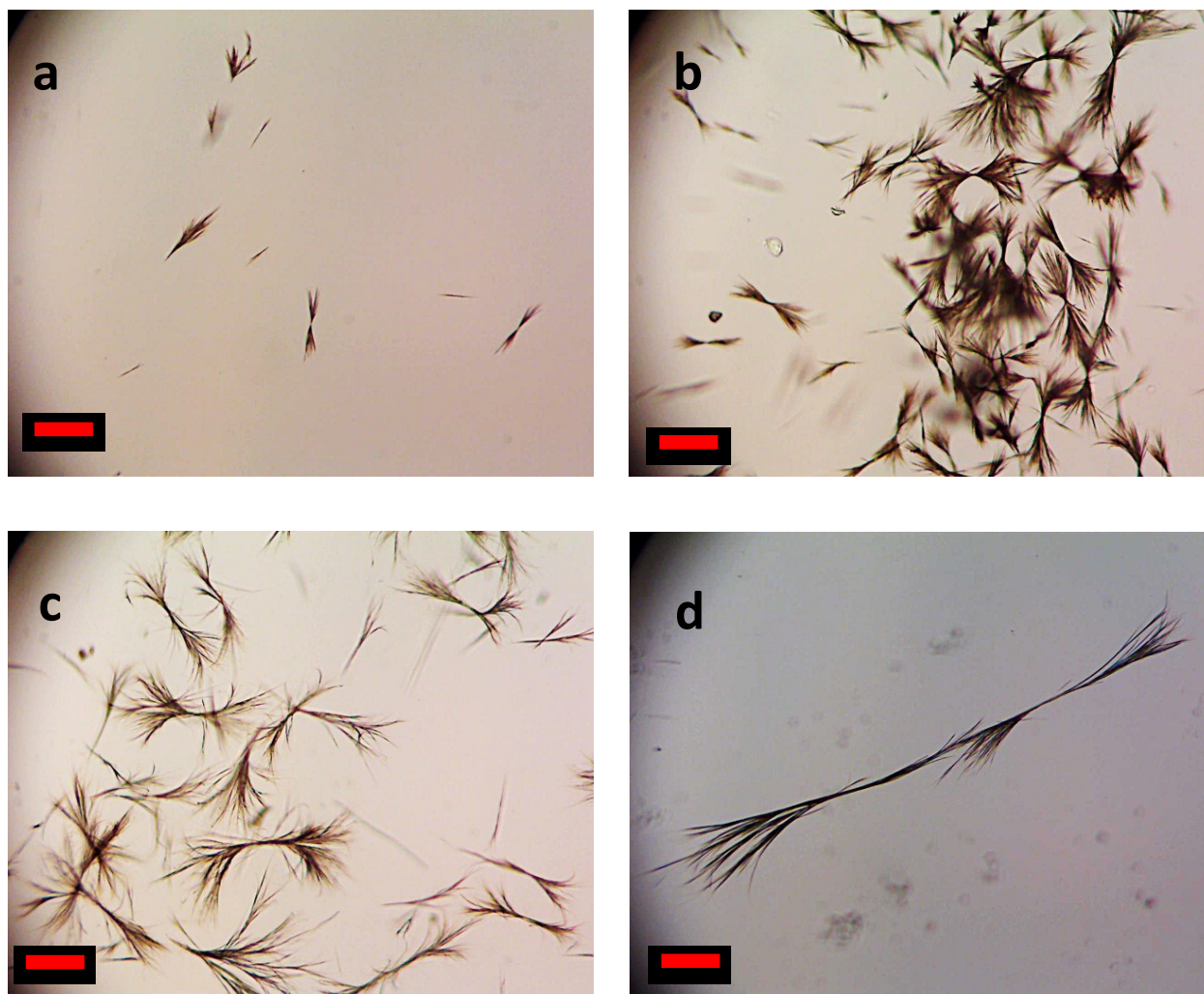


**Figure S9.** Optical microscopy images of 4F9AC branched microcrystals grown using increasing concentrations of 1-dodecanol with  $[\text{SDS}] = 7 \text{ mM}$ ,  $[\text{H}_3\text{PO}_4] = 3.5 \text{ M}$ , and the initial  $[\textit{tert}\text{-butyl-4F9AC}] = 0.3 \text{ mM}$ . (a)  $[\text{1-dodecanol}] = 0 \text{ mM}$ . (b)  $[\text{1-dodecanol}] = 1 \text{ mM}$ . (c)  $[\text{1-dodecanol}] = 3 \text{ mM}$ . (d)  $[\text{1-dodecanol}] = 5 \text{ mM}$ . Scale bars =  $150 \text{ }\mu\text{m}$ .



ESI- Movie 1 : <https://www.youtube.com/watch?v=QJWWgePkEHo>

ESI- Movie 2 : <https://www.youtube.com/watch?v=QEI-MA6TOj4>

ESI- Movie 3 : <https://www.youtube.com/watch?v=OL8WDxSwk74>

ESI- Movie 4 : <https://www.youtube.com/watch?v=FOe1NPDyFzo>